

<https://doi.org/10.1038/s43856-024-00612-w>

MHC class II genotypes are independent predictors of anti-PD1 immunotherapy response in melanoma

Check for updates

Arne Claeys ^{1,2} & Jimmy Van den Eynden ^{1,2}

Abstract

Background Immune checkpoint blockade is a highly successful anti-cancer immunotherapy. Both CTLA4 and PD1 checkpoint blockers are clinically available for melanoma treatment, with anti-PD1 therapy reaching response rates of 35–40%. These responses, which are mediated via neoantigen presentation by the polymorphic MHC complex, are hard to predict and the tumor mutation burden is currently one of the few available biomarkers. While MHC genotypes are expected to determine therapy responses, association studies have remained largely elusive.

Methods We developed an overall MHC genotype binding score (MGBS), indicative of a patient's MHC class I (MHC-I) and class II (MHC-II) neoantigen binding capacity and solely based on the germline MHC-I (MGBS-I) and MHC-II (MGBS-II) genotypes. These scores were then correlated to survival and clinical responses following anti-PD1 immunotherapy in a previously published dataset of 144 melanoma patients.

Results We demonstrate that MGBS scores are TMB-independent predictors of anti-PD1 immunotherapy responses in melanoma. Opposite outcomes were found for both MHC classes, with high MGBS-I and MGBS-II predicting good and bad outcomes, respectively. Interestingly, high MGBS-II is mainly associated with treatment response failure in a subgroup of anti-CTLA4 pretreated patients.

Conclusions Our results suggest that MGBS, calculated solely from the MHC genotype, has clinical potential as a non-invasive and tumor-independent biomarker to guide anti-cancer immunotherapy in melanoma.

Plain language summary

Many cancer patients are successfully treated with immunotherapy, which boosts the immune system to eliminate cancer cells. While this therapy is successful in around half of skin cancer melanoma patients, it is currently hard to determine in advance which patients respond well. Immune cells react to tumor proteins that are presented at the cancer cell surface by molecules called MHC. These are unique for every patient. We aimed to determine whether the ability of MHC to bind to tumor proteins determines how well therapy works and developed a new way to quantify this interaction. Surprisingly, less ability for tumor proteins to bind to the unconventional class II MHC resulted in better clinical outcome in patients with melanoma. Our results provide new understanding of tumor-immune interaction and the new method may help determine which patients with melanoma will respond to therapy.

Immune checkpoints are regulatory pathways that attenuate anti-tumoral T cell responses^{1,2}. The first clinical successes with immune checkpoint blockade (ICB) immunotherapy were achieved with the CTLA4 (cytotoxic T lymphocyte-associated protein 4) blocking antibody ipilimumab, followed by the anti-PD1 (programmed cell death 1) antibody nivolumab in advanced metastatic melanoma^{3,4}. Response rates of anti-PD1 treatment (35–40%) are superior to anti-CTLA4 (15%)¹, which is likely related to different mechanisms of action. Anti-CTLA4 interferes with T cells and antigen presenting dendritic cells during initial activation of anti-tumor T cells in lymph nodes, while anti-PD1 directly blocks the interaction between T cells and cancer cells, which express the PD1 ligand (PD-L1)^{1,2}. Patients failing to respond to ipilimumab have been successfully treated with nivolumab, a sequence that has been shown superior to the opposite

approach (first nivolumab)⁵ and, more recently, combinatorial treatment was found better than monotherapy (response rates around 50%)^{6,7}.

Despite these successes, ICB responses are hard to predict, and the TMB is currently one of the few FDA-approved biomarkers in different cancer types (the other being PD-L1 expression and microsatellite instability)^{8–15}. Indeed, anti-tumoral responses are mediated by neoantigens, small, mutated peptides that are presented to CD8⁺ cytotoxic T cells at the cancer cell membrane by the class I major histocompatibility complex (MHC-I). This explains why the best ICB responses are observed in mutagen-exposed tumors (e.g., melanoma, lung cancer) with a high TMB and hence high expected neoantigen load. As the presentability of a mutated peptide by MHC-I is determined by a patient's MHC genotype, these genotypes have the potential to predict ICB responses. However, association

¹Department of Human Structure and Repair, Unit of Anatomy and Embryology, Ghent University, Ghent, Belgium. ²Cancer Research Institute Ghent, Ghent University, Ghent, Belgium. ✉e-mail: jimmy.vandeneinden@ugent.be

studies remained largely elusive, which is likely related to the low allele frequency in combination with the complexity of the MHC genotype. Indeed, each MHC-I genotype is determined by a rather unique combination of 6 highly polymorphic alleles (2 *HLA-A*, *HLA-B* and *HLA-C* alleles). While some associations have been described between more frequent MHC-I allele groups (e.g., B44 and B62) and ICB responses¹⁶, statistical power is lacking for the majority of (infrequent) alleles. Indeed, a simple power calculation indicates that more than 10,000 samples would be required to detect a hazard ratio (HR) of 2 (or lower) for alleles with a 0.1% allele frequency (Supplementary Fig. 1). Furthermore, even if the required data sizes would be reached, these studies only focus on the presence (or absence) of 1 allele, ignoring how the combined effect with the other 5 alleles of the MHC-I genome affects treatment responses.

Even less is known about putative associations between ICB responses and the more complex MHC class II (MHC-II) genotype, which is determined by 10 different alleles (*HLA-DPA1*, *HLA-DPB1*, *HLA-DQA1*, *HLA-DQB1* and *HLA-DRB1* genes). While MHC-II is generally expressed by antigen presenting cells (e.g., dendritic cells) and responsible for neoantigen presentation to CD4+ helper T cells, recent evidence suggests that cancer cells can express MHC-II directly^{17,18}. Interestingly, high MHC-II expression has been associated with positive responses to ICB¹⁹.

Here, we developed a simple quantitative indicator of a patient's germline-determined overall MHC-I and MHC-II presentability, referred to as MGBS-I (MHC-I Genotype Binding Score) and MGBS-II, respectively. These scores were then correlated to anti-PD1 outcomes in 144 melanoma patients of a previously published study. Weak positive correlations were found between outcome and MHC-I presentability, but, strikingly, opposite and strong negative correlations were observed with MHC-II presentability, particularly in a subgroup of anti-CTLA4 pretreated patients. Our results shed new light on the immunomodulatory role of MHC-II and suggest that MHC genotypes have potential as a tumor-agnostic response biomarker in anti-PD1 treated melanoma.

Methods

Data download and processing

The analysis presented in the current publication is based on genomic and clinical data derived from 144 melanoma patients as published in a previous study¹⁹. The Whole Exome Sequencing (WES) and RNA-Seq FASTQ files of this study were derived from dbGaP (<https://www.ncbi.nlm.nih.gov/gap/>), under phs000452.v3.p1 (https://www.ncbi.nlm.nih.gov/projects/gap/cgi-bin/study.cgi?study_id=phs000452.v3.p1). Clinical response data were downloaded from supplementary table 4, accessible at https://static-content.springer.com/esm/art%3A10.1038%2F41591-019-0654-5/MediaObjects/41591_2019_654_MOESM4_ESM.xlsx¹⁹.

Additional WES and RNA-Seq datasets, as reported in Supplementary Fig. 4 and Supplementary Fig. 8, were obtained from the European Nucleotide Archive (<https://www.ebi.ac.uk/ena>; accession numbers PRJNA307199/PRJNA343789²⁰, PRJEB23709²¹ and PRJNA359359/PRJNA356761²²) and dbGaP (accession numbers phs000452.v3.p1¹⁰, phs000980.v1.p1⁸, and phs001041.v1.p1⁹). Clinical data were obtained from the published supplementary information from the corresponding studies.

All data were accessed and used in strict accordance with dbGaP's Data Use Certification (DUC) requirements. The data in dbGaP were originally collected and submitted by the primary investigators of the source studies, who certified that appropriate informed consent was obtained from all participants and ethical oversight and approval were provided by the respective Institutional Review Boards (IRBs) of the contributing institutions.

Consensus HLA allele frequencies for a Caucasian American and African American population were constructed based on 18 different datasets from the Allele Frequency Net Database (<http://www.allelefrequencies.net/>)²³. Results from different datasets were combined into a single consensus frequency by first mapping all listed alleles to the corresponding G-groups, trimming them at second-field resolution and

subsequently calculating the average frequency per allele, weighted by each study's sample size.

MHC genotyping

MHC genotyping was performed on normal control blood-derived WES files using Optitype v1.3.5 for MHC-I (*HLA-A*, *HLA-B* and *HLA-C*) and HLA-HD v1.3 for MHC-II (*HLA-DPA1*, *HLA-DPB1*, *HLA-DQA1*, *HLA-DQB1* and *HLA-DRB1*), following previously published recommendations²⁴. Both tools were run using default parameters. For one of the validation datasets (Gide et al.²¹), no WES files from normal control samples were available and arcasHLA v0.2.0 was applied on tumor derived RNA-Seq files.

Calculation of MGBS-I and MGBS-II

One million random 9-meric and 15-meric peptides were first generated by randomly sampling 9×/15× from all 20 amino acids with repetition. HLA affinities of these peptides were calculated using NetMHCpan-4.0 for MHC-I (9-mers) and NetMHCIIpan-3.2 for MHC-II (15-mers)^{25,26}. MGBS-I was defined as the average proportion of MHC binders (defined as peptides with Kd <500 nM) for the 6 patient-specific germline MHC-I alleles (2 copies of *HLA-A*, *HLA-B* and *HLA-C* genes). Similarly, MGBS-II was defined as the average proportion of peptides binding to the specific HLA-DP, HLA-DQ and HLA-DR heterodimers in a patient, given the patient's 10 germline MHC-II alleles (2 copies of *HLA-DPA1*, *HLA-DPB1*, *HLA-DQA1*, *HLA-DQB1* and *HLA-DRB1* genes). MGBS-d was defined as the difference between MGBS-I and MGBS-II after rank normalizing both scores. This normalization was performed to account for different scales of both scores.

Gene expression quantification

Gene expression was quantified using RSEM (v1.3.3) with the STAR (v2.7.10b) aligner. First, a STAR-compatible reference transcriptome was prepared from the GRCh38.d1.vd1 human genome assembly and GENCODE v39 annotation using *rsem-prepare-reference*. Next, reads were aligned to the reference transcriptome with STAR and expression was quantified at the gene level using *rsem-calculate-expression*. Downstream analyses were based on the resulting TPM counts.

When data from different studies were directly compared (i.e., in Supplementary Fig. 8) batch effects were first corrected using the *ComBat-seq* method from the *sva* R package (v3.50), without including any additional covariates. *ComBat-Seq* was applied to raw RNA-Seq counts. Resulting counts were then converted to TPM (transcripts per million) values using the *convertCounts* function from the *DGEobjutils* R package (v1.0.6).

Survival analysis

Survival analysis was performed using the R packages *survminer* and *survival* in default settings. Kaplan-Meier analyses were plotted using the *survfit* and *ggsurv* functions with calculation of *P* values using a log rank test. Univariate and multivariate Cox regression analyses were performed using the *coxph* function.

Survival power analysis was performed using the *ssizeCT.default* function from the *powerSurvEpi* R package.

Multivariate analyses

The following variables were obtained from the supplementary information of the respective studies (when available): TMB (defined as the total number of non-synonymous mutations), *HLA* and *B2M* LOH, LDH serum concentration, ploidy, purity, tumor heterogeneity (defined as the proportion of subclonal mutations, i.e., mutations with a cancer cell fraction <0.8) and lymph node metastatic status. *PD-L1* (*CD274*) was derived from the gene expression data and cytolytic activity was defined as the geometric mean of *GZMA* and *PRFI*²⁷. MHC-I and MHC-II expression values were calculated using the ssGSEA method from the R package *GSEA* on the MHC-I and MHC-II gene sets, as defined by Liu et al.¹⁹. Additionally, we calculated total

MHC-I and MHC-II zygosity, defined as the total number of different alleles (maximal 6 and 10 for MHC-I and MHC-II respectively) from the MHC genotypes.

To associate these variables with clinical responses (defined as non-progressive patients, RECIST criteria), all variables were z-normalized and fed in a feed-forward multivariate logistic regression model in a stepwise manner using the R *stats* package (*step* function). Variables that did not contribute significantly to the resulting model ($P > 0.05$) were iteratively excluded until all remaining variables contributed significantly. Predicted responders were defined based on a probability cut-off of 0.5 from the respective logistic regression model. A similar feed-forward approach was implemented to determine the variables contributing to a Cox regression model.

Differential gene expression and gene set enrichment analysis

Differential gene expression analysis was performed using Limma version 3.54, with gene-level counts imported from RSEM output files using the *tximport* (v1.26) package. Mean-variance relationship was modeled using voom precision weights. P values were calculated using a moderated t-statistic as reported by Limma. Gene set enrichment analysis (GSEA) was performed using the R *fgsea* package (*fgseaMultilevel* function, default parameters) with ranking based on the P values. Hallmark gene sets were downloaded from the Molecular Signatures Database (MSigDB) v7.5.1.

Statistics and reproducibility

The R statistical package (v4.0) was used for all data processing and statistical analysis. Details on the statistical tests used in this study are reported in the respective sections. P values less than 0.05 were considered significant for individual tests. For multiple comparisons, false discovery rate (FDR) corrections were performed using the Benjamini-Hochberg method.

Reporting summary

Further information on research design is available in the Nature Portfolio Reporting Summary linked to this article.

Results and discussion

MHC-II binding capacity is adversely associated with outcome to anti-PD1 immunotherapy in melanoma patients

Previous association studies between MHC genotypes and ICB outcome are limited by their single allele focus and the lack of statistical power (Supplementary Fig. 1). To circumvent both problems, we developed a simple indicator of a patient's germline-determined overall MHC-I presentability, called MGBS-I (MHC-I Genotype Binding Score). MGBS-I is the probability of a patient-specific MHC-I complex to bind a random 9-mer peptide, as calculated for 1 million different peptides and considering all 6 HLA alleles (Fig. 1a). We then evaluated MGBS-I as an ICB predictor in a previously published dataset of 144 melanoma patients that were treated with the anti-PD1 ICB nivolumab, which is currently, to our knowledge, the largest single-study ICB melanoma dataset with available genomic and clinical follow-up data¹⁹. As expected, the 72 (50%) patients with the highest TMB (>250 mutations, median value) had better overall survival than the 72 patients with the lowest TMB ($P = 0.0012$, log rank test; Fig. 1b). Interestingly, when patients were stratified based on their MGBS-I, the 50% patients with the strongest binding scores (MGBS-I > 0.016) showed a trend towards better survival than patients with the weakest binding scores ($P = 0.055$; Fig. 1c, d). Notably, responses became stronger when more stringent criteria were used to define strong binders (i.e., based on 75th, 90th or 95th percentiles; Fig. 1d, Supplementary Fig. 2). These findings are in agreement with a previously suggested association between poor ICB therapy outcome and weaker MHC-I presentability of peptides translated from a set of cancer driver mutations²⁸.

We then extended our methodology to the more complex MHC-II genotype, which is determined by 10 different alleles (Fig. 1a). Strikingly, the 50% patients with the highest MGBS-II scores (MGBS-II > 0.12) had significantly worse survival after ICB as compared to the group of patients with

the lowest MGBS-II scores ($P = 0.0067$; Fig. 1d, e). As for MGBS-I, survival differences were more pronounced when more stringent criteria were used to define strong binders (Fig. 1d, Supplementary Fig. 2). Interestingly, no correlation was found between TMB, MGBS-I and MGBS-II, suggesting these are independent biomarkers (Supplementary Fig. 3). This was confirmed by a Cox proportional hazard regression analysis, which indicated TMB-independent associations with survival for both MGBS-I (HR = 0.64, $P = 0.065$) and MGBS-II (HR = 1.7, $P = 0.032$; Fig. 1f). Given the opposite survival associations, we then focused on the difference between MGBS-I and MGBS-II (after normalizing both scores, see *Methods*) and defined this difference as MGBS-d. A strong survival difference was observed when comparing the 50% patients with the highest MGBS-d scores to the patients with the lowest scores ($P = 6.4 \times 10^{-4}$; Fig. 1g), a finding that was again independent of TMB (HR = 0.50, $P = 0.0048$; multivariate analysis considering TMB; Fig. 1f). Interestingly, patients that responded to therapy (i.e., classified as non-progressive following RECIST criteria) had significantly lower MGBS-II scores ($P = 0.037$) and MGBS-d scores ($P = 0.0067$) as compared to non-responding patients (Fig. 1h, i).

We then aimed to validate our findings on 3 independent anti-PD1 treated melanoma datasets with available clinical and molecular data from Hugo et al.²⁰ ($n = 37$), Gide et al.²¹ ($n = 36$) and Riaz et al.²² ($n = 68$). The first 2 studies confirmed the association between lower-than-median MGBS-II and better survival, although this was only significant for the Hugo study ($P = 0.014$) and not the Gide study ($P = 0.10$; Supplementary Fig. 4). Interestingly, RECIST clinical responses were significantly worse ($P = 0.0076$, Chi-square test) for patients with higher MGBS scores for the latter study. While similar, though non-significant patterns were observed in anti-PD1 lung cancer patients⁸, no correlation was observed between outcome and MGBS in the Riaz study nor in 2 studies of anti-CTLA4 treated patients^{9,10} (Supplementary Fig. 4).

As an alternative strategy to MGBS, we explored the predictive value of absolute MHC-I and MHC-II neoantigen burden (NeoAgB). Both metrics showed a strong positive association with survival ($P = 3.9 \times 10^{-3}$ and $P = 1.3 \times 10^{-3}$ for MHC-I and MHC-II respectively), in line with the findings from previous studies²⁹, but opposite to what we observed using MGBS-II (Supplementary Fig. 5). The strong correlation with TMB (Supplementary Fig. 3) suggests that these associations are secondary to TMB, resulting in a masking of the negative MHC-II association. Indeed, after normalizing NeoAgB to TMB (referred to as the normalized NeoAgB), similar but weaker, non-significant associations with survival were observed as for MGBS (Supplementary Fig. 5). We speculate that the reason for these weaker signals is related to the relatively few mutations (median 250) that are used to calculate NeoAgB on the one hand (i.e., relatively high statistical uncertainty) and the tumor evolutionary selection processes that could have shaped the mutational landscape on the other hand.

MHC-II genotypes and MHC-II expression independently predict clinical response to anti-PD1 therapy in anti-CTLA4 pretreated melanoma patients

A subgroup of 60 patients received prior ipilimumab ICB immunotherapy and this prior treatment has been recently associated with differences in the tumor microenvironment, affecting the predictive features of anti-PD1 responses³⁰. Therefore, we hypothesized that the MHC genotypes could underlie these differences. As expected, survival probability was lower for ipilimumab-pretreated patients compared to treatment naive patients ($P = 0.028$, Fig. 2a). Interestingly, the TMB effect was restricted to pre-treatment naive patients ($P = 0.0061$), while the MGBS-II association was only observed in patients that received prior ipilimumab treatment ($P = 0.0024$; Fig. 2b). A Cox multivariate analysis confirmed these results, with TMB and MGBS-II being independently associated with survival in treatment naive patients ($P = 0.0073$) and ipilimumab patients ($P = 0.0089$), respectively (Fig. 2c).

Our findings shed new light on previous studies suggesting an influence of prior anti-CTLA4 treatment on the predictive features of anti-PD1 responses^{19,30}. In this regard, Liu et al. developed a logistic regression model

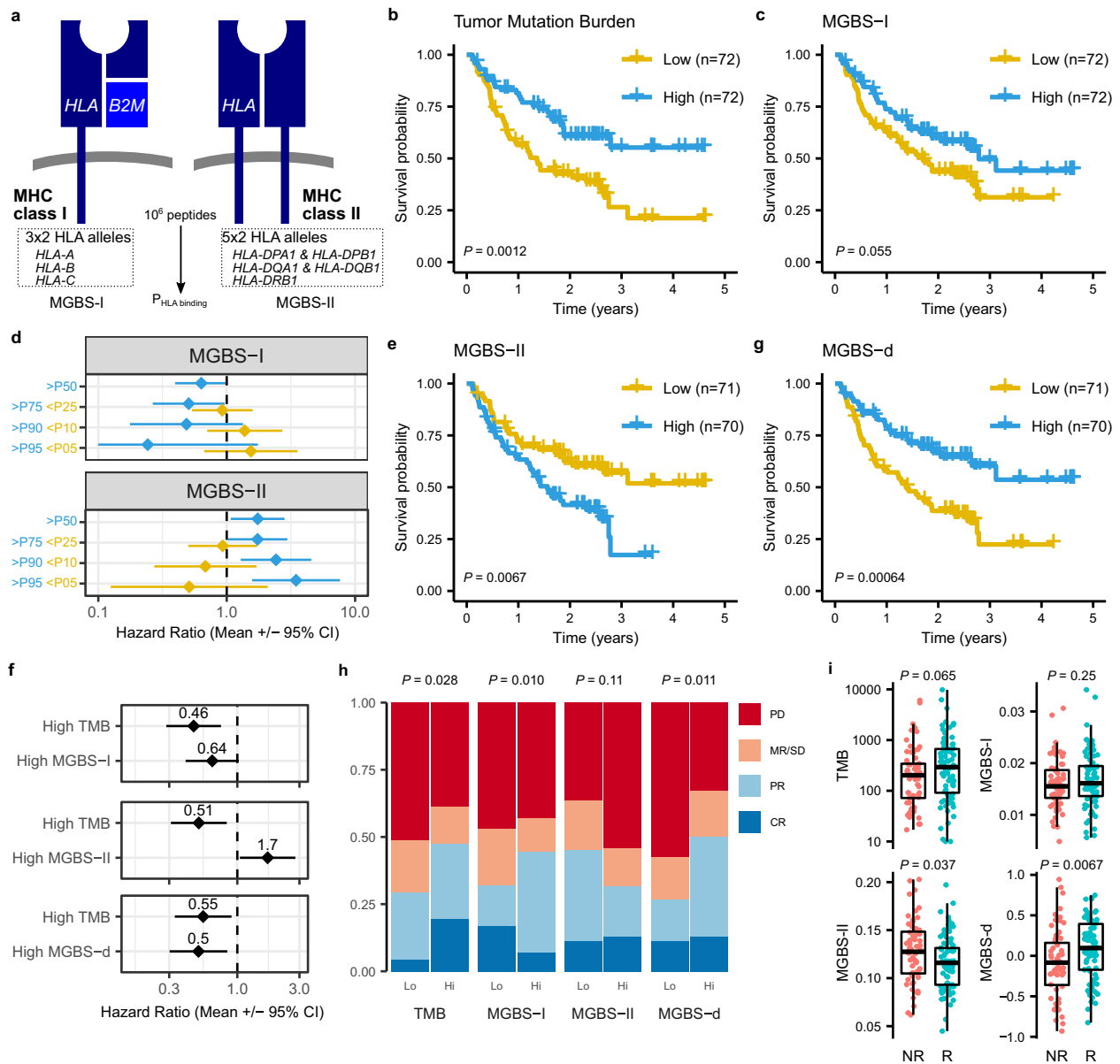


Fig. 1 | A quantitative MHC genotyping approach to predict melanoma anti-PD1 immunotherapy responses. a An MHC Genotype Binding Score (MGBS) was developed to quantify the germline-specific Major Histocompatibility Complex (MHC) peptide binding capacity. MGBS is the HLA binding probability of all 6 class I alleles (MGBS-I) or 10 class II alleles (MGBS-II), calculated for 1 million random peptides. **b–g** Survival analysis of a set of previously published melanoma patients that were treated with nivolumab ($n = 144$). Patients were stratified in 2 groups based on the median Tumor Mutation Burden (TMB), MGBS-I, MGBS-II and MGBS-d (representing the difference between MGBS-I and MGBS-II, see *Methods*). Kaplan-Meier analysis with log rank test P values shown in (**b**, **c**, **e** and **g**). **d** Forest plots indicating hazard ratio $\pm 95\%$ confidence intervals as determined from a univariate

Cox regression analysis using different threshold to group patients in top and bottom percentiles (y-axis labels) and taking the interpercentile group of patients as a reference. See Supplementary Fig. 2 for corresponding Kaplan-Meier plots. **f** Forest plots indicating hazard ratio $\pm 95\%$ confidence intervals as determined from a multivariate Cox regression analysis as indicated. **h** Stacked bar plots indicating clinical response (as determined using RECIST criteria) for the 4 variables as indicated. P values calculated using two-sided Chi-squared test. **i**. Boxplots comparing TMB/MGBS scores between responders (R) and non-responders (NR). Boxplots represent median values and lower or upper quartiles with whiskers extending to 1.5 times the interquartile range. P values calculated using two-sided Wilcoxon rank sum test.

that predicted clinical responses in patients that received prior anti-CTLA4 therapy based on MHC-II expression, serum LDH levels and lymph node metastases¹⁹. As MHC genotypes were not directly considered in the Liu study, we redeveloped this regression model, using an unbiased feed-forward-selection approach (see *Methods*) that included several previously described biomarkers (e.g., *PD-L1* expression, *B2M* LOH, MHC zygosity) and the 3 MGBS metrics (Fig. 3 and Supplementary Fig. 6). Strikingly, responses of the pretreated patient group were predicted highly accurately (mean AUC = 0.87, calculated from 100 repetitions of a 5-fold cross-validation approach) by a combination of high MHC-II expression

($P = 0.0070$), low MGBS-II scores ($P = 0.013$), *B2M* LOH ($P = 0.028$) and tumor heterogeneity ($P = 0.028$; Fig. 3a, b and Supplementary Fig. 6). Notably, MGBS-II had the highest predictive value of all variables in a univariate setting (mean AUC = 0.76) and exclusion of MGBS-II from the multivariate model reduced the mean AUC from 0.87 to 0.79, similar to what was reported by Liu et al. when MHC genotypes were not considered¹⁹ (Fig. 3b). When patients were subsequently stratified using model predictions, large survival differences were observed between predicted responders and non-responders in the ipilimumab pretreated subgroup ($P < 1.0e-4$; Fig. 3c). Interestingly, following the same statistical approach in the

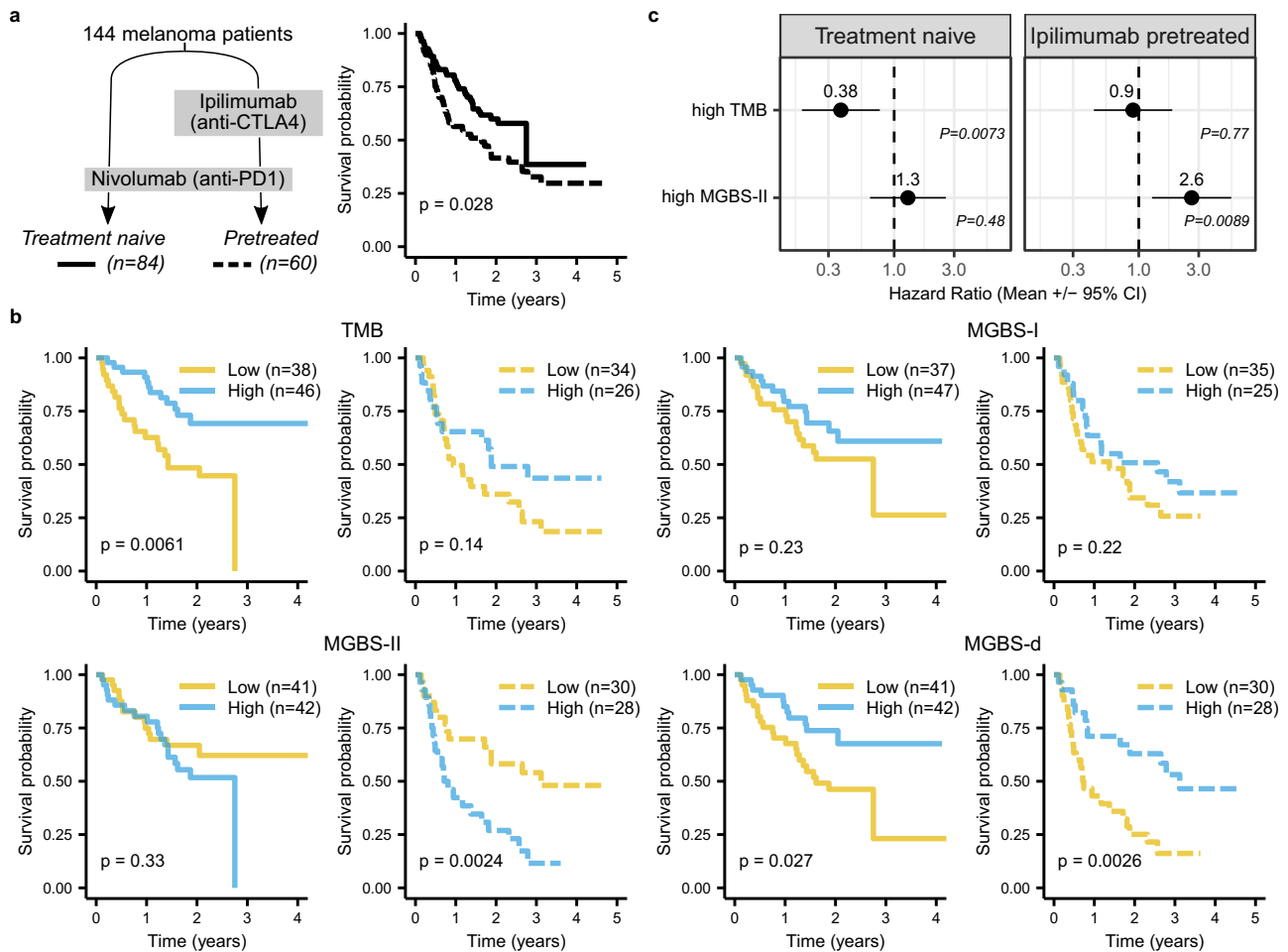


Fig. 2 | Ipilimumab pretreatment-dependent survival analysis. **a** A subgroup of 60 patients was pretreated with ipilimumab before receiving nivolumab treatment as indicated. Kaplan-Meier plot compares survival between pretreated (n = 60; dashed curve) with treatment naive (n = 84; solid curve) patients. **b** Kaplan-Meier plots comparing patients with high to low TMB/MGBS-I/MGBS-II/MGBS-d for treatment naive (left, solid curves) and pretreated (right, dashed curves) patients, as

indicated. *P* values calculated using log rank test. **c**, Forest plots indicating hazard ratio \pm 95% confidence intervals as determined from a multivariate Cox regression analysis using TMB and MGBS-II as variables, after stratifying both patient groups following their pretreatment as indicated. *TMB* Tumor Mutation Burden; *MGBS-I/MGBS-II/MGBS-d* MHC Genotype Binding Score for MHC-I, MHC-II and the difference, respectively.

pretreatment-naive group of patients resulted in the best predictions (AUC = 0.78) using a combination of tumor heterogeneity ($P = 0.0087$), ploidy ($P = 0.011$) and MGBS-I ($P = 0.024$). A similar feed-forward multivariate Cox regression approach resulted in the selection of tumor purity (HR = 2.7, $P = 0.010$) and heterogeneity (HR = 4.8, $P = 1.0e-4$) in the pretreatment-naive patients and MGBS-II (HR = 4.3, $P = 9.6e-4$) in the pretreated patients (Supplementary Fig. 7).

The independent association between MHC-II expression and the MHC-II genotype (quantified using MGBS-II) with patient responses suggests an important role of the MHC-II complex in modulating responses to anti-PD1 immunotherapy. While MHC-II expression has been suggested as a biomarker for anti-PD1 outcome previously^{19,29,31}, our study is, to our knowledge, the first to demonstrate a role of the MHC-II genotype-determined HLA binding potential. In light of this putative MHC-II immunomodulatory role, we evaluated the predictive capacity of the combined MGBS-II and MHC-II expression values, using a logistic regression model developed on the Liu ipilimumab pretreated patient data. As expected, predicted responders had better survival than predicted progressors in the Liu data ($P = 9.7e-04$ and $P = 0.0098$ in the overall and pretreated groups, respectively). Interestingly, when this model was applied on the 3 independent anti-PD1 melanoma validation studies, significant survival differences were now observed in the Gide data ($P = 0.043$; 22/35 predicted responders). A similar trend was observed in

the Hugo data ($P = 0.19$; 14/26 predicted responders) while the differences between predicted responders and progressors were rather marginally in the Riaz data ($P = 0.52$; Supplementary Fig. 8a). To better understand these differences, we compared the Cox HRs of the evaluated biomarkers between all 4 studies. A remarkable difference was noted between the pretreated patients of the Liu and the Riaz data (Supplementary Fig. 4b and 8b). Indeed, while the HRs in the treatment naive groups were strongly correlated (Pearson’s $r = 0.87$, $P = 1.1e-04$), no correlation was observed in the ipilimumab pretreated group. Most remarkable, a lack of survival association was observed with MHC-II expression, PD-L1 expression and TMB, with the latter even trending towards an opposite association than what is generally expected (HR = 2.3, $P = 0.10$). These results suggest that the Riaz patients lack the MHC-II immunomodulation seen in the other studies. The discrepancies between the ipilimumab pretreated cohorts from both studies point towards differences in patient selection procedures. This is further supported by a remarkable difference in tumor heterogeneity between the Liu and the Riaz study ($P = 1.1e-07$, Kruskal-Wallis rank sum test; Supplementary 8c).

TMB and MHC-II binding properties are inversely correlated to gamma interferon activity

To better understand the mechanism underlying these genotype-dependent responses, we searched for enriched gene sets following a

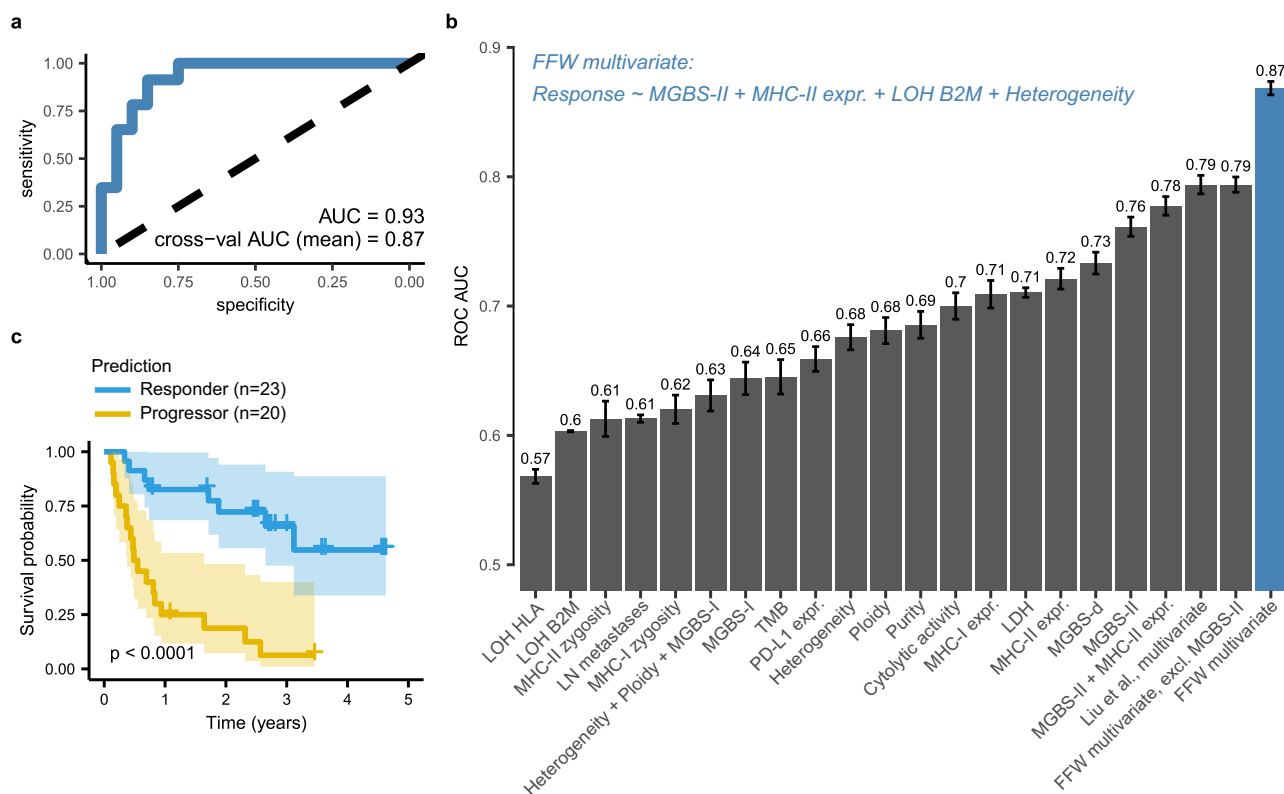


Fig. 3 | A multivariate logistic regression model to predict clinical responses in ipilimumab pretreated patients. Previously suggested biomarkers were associated with clinical responses (patients classified as non-progressive, RECIST criteria) in ipilimumab pretreated patients. A feed-forward (FFW) multiple logistic regression approach (see *Methods*) resulted in the selection of 4 variables as indicated. **a** Receiver Operating Curve (ROC) with indication of the Area Under the Curve (AUC). Mean AUC was calculated from 100 repetitions of a 5-fold cross validation

approach. **b** Bar plots indicating mean AUC values for all variables, the FFW multivariate model with or without exclusion of MGBS-II and a 3-variable model suggested by ref. 19. (i.e., MHC-II expr., LDH and LN metastasis). Error bars represent 95% confidence intervals. **c** Kaplan-Meier survival plots for predicted responders and non-responders following the FFW multivariate model. Log rank *P* value indicated. MGBS-II, MHC-II Genotype Binding Score.

differential gene expression analysis between patients with low and high TMB/MGBS-I/MGBS-II/MGBS-d. Interestingly, the strongest enrichments were found for the *Hallmark interferon (IFN) gamma response* gene set in tumors characterized by a high TMB (*P*_{adj} = 1.1e-21) as well as a low MGBS-II (*P*_{adj} = 6.4e-30; Fig. 4), in line with the well-established role of IFN gamma in modulating ICB responses³². To determine whether TMB and MGBS resulted in differential responses of the tumor microenvironment during prior ipilimumab treatment, we compared the gene set enrichment results between patients with and without pretreatment. While we did not observe any clear differences in *IFN gamma response* enrichment between pretreatment groups, a striking difference was noted for cell cycle-related pathways such as *E2F targets* and *G2M checkpoint* (Supplementary Fig. 9). Indeed, while these pathways were always strongly enriched in patients with high TMB (*P*_{adj} < 1e-5 in all conditions), they were only enriched in pretreatment naive patients with high MGBS-I scores (*P*_{adj} = 3.7e-24 for *E2F targets*; *P*_{adj} = 3.3e-16 for *G2M checkpoint*) and pretreated patients with high MGBS-II scores (*P*_{adj} = 6.7e-11 for *E2F targets*; *P*_{adj} = 2.4e-10 for *G2M checkpoint*). This was also evident when focusing on MGBS-d, which was mainly associated with an enrichment of these pathways in treatment-naive patients (Supplementary Fig. 9). These results suggest that differential modulations of the TME by the MHC class I and class II genotypes are responsible for the observed treatment responses.

Conclusion

Our study demonstrates that the HLA binding capacity of the MHC genotype, quantified using a simple metric, has potential as a new

biomarker in anti-PD1 treated melanoma. The value of this putative biomarker remains to be determined in larger clinical studies and other cancer types where ICB has been proven successful. Given the strong association we observed between the MHC class II genotype and responses to sequential ICB therapy, our metric could have clinical relevance in patients receiving combined anti-CTLA4 and anti-PD1 treatment. An important advantage for such studies and future clinical applications is that MHC genotyping does not require a tumor biopsy but could be performed on a simple blood sample. Additionally, contrary to the TMB and related neoantigen burden, the MHC genotype is a static variable that is not influenced by prior mutational selection or immunoeediting processes, which can differently affect clinical responses to ICB therapy.

Data availability

This study is completely based on previously published genomic and clinical data, available via dbGAP (<https://www.ncbi.nlm.nih.gov/gap/>; accession numbers phs000452.v3.p1 phs000452.v3.p1, phs000980.v1.p1 and phs001041.v1.p1) and the European Nucleotide Archive (<https://www.ebi.ac.uk/ena/>; accession numbers PRJNA307199, PRJNA343789, PRJEB23709, PRJNA359359 and PRJNA356761). Downstream data are provided in Supplementary Data 1. Source data for the figures are available at <https://doi.org/10.5281/zenodo.12517305> (data/MHC_immunotherapy.RData)³³.

Code availability

The code used to produce the results described in this manuscript is available at <https://doi.org/10.5281/zenodo.12517305>³³.

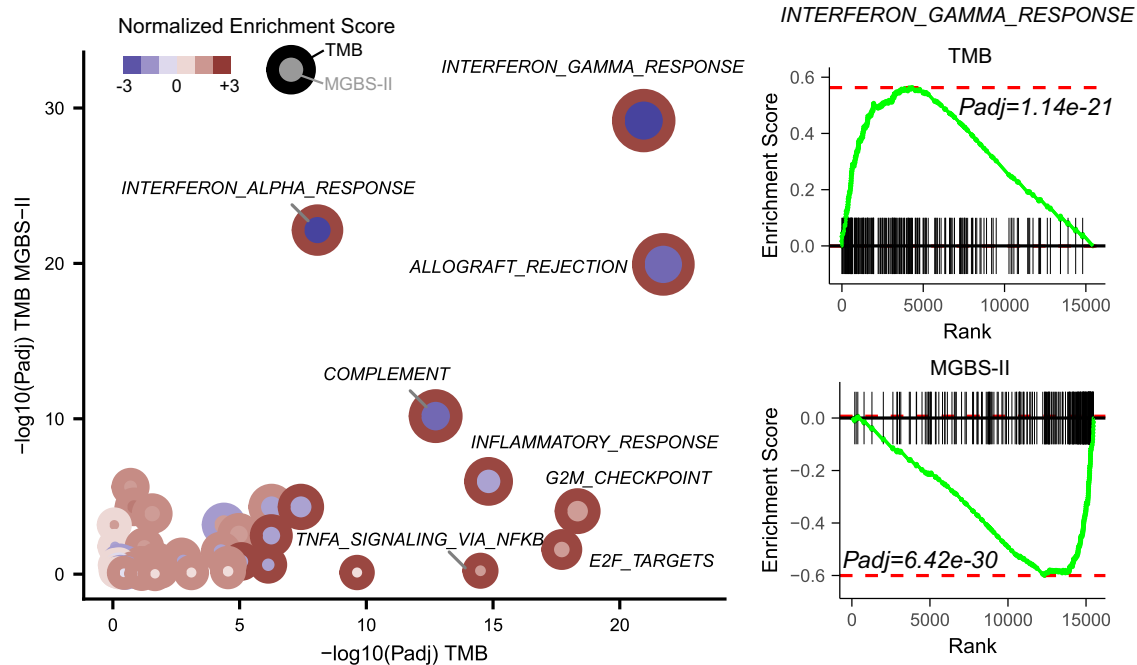


Fig. 4 | Hallmark gene set enrichment analysis of genes differentially expressed between patients with high and low TMB and MGBS-II. Differential gene expression was determined between patients with low and high TMB and MGBS-II (median value cut-offs) and a preranked Hallmark gene set enrichment analysis was performed. Plot compares enrichment *Padj* values ($-\log_{10}$ scale) between TMB and

MGBS-II for all 50 Hallmark gene sets. Most enriched gene sets labeled. Normalized enrichment scores indicated by point fill and border colors, respectively, as indicated by color legend on top left. Right panels show the *interferon gamma response* gene set running score plots for TMB and MGBS-II. TMB tumor mutation burden, MGBS-I/MGBS-II, MHC-I/II genotype binding score.

Received: 3 August 2023; Accepted: 17 September 2024;
Published online: 30 September 2024

References

- Ribas, A. & Wolchok, J. D. Cancer immunotherapy using checkpoint blockade. *Science* **359**, 1350–1355 (2018).
- Pardoll, D. M. The blockade of immune checkpoints in cancer immunotherapy. *Nat. Rev. Cancer* **12**, 252–264 (2012).
- Topalian, S. L. et al. Survival, durable tumor remission, and long-term safety in patients with advanced melanoma receiving nivolumab. *J. Clin. Oncol.* **32**, 1020–1030 (2014).
- Hodi, F. S. et al. Improved survival with ipilimumab in patients with metastatic melanoma. *N. Engl. J. Med.* **363**, 711–723 (2010).
- Weber, J. S. et al. Sequential administration of nivolumab and ipilimumab with a planned switch in patients with advanced melanoma (CheckMate 064): an open-label, randomised, phase 2 trial. *Lancet Oncol.* **17**, 943–955 (2016).
- Hodi, F. S. et al. TMB and inflammatory gene expression associated with clinical outcomes following immunotherapy in advanced melanoma. <https://doi.org/10.1158/2326-6066.CCR-20-0983> (2021).
- Larkin, J. et al. Five-year survival with combined nivolumab and ipilimumab in advanced melanoma. *N. Engl. J. Med.* **381**, 1535–1546 (2019).
- Rizvi, N. A. et al. Cancer immunology. Mutational landscape determines sensitivity to PD-1 blockade in non-small cell lung cancer. *Science* **348**, 124–128 (2015).
- Snyder, A. et al. Genetic basis for clinical response to CTLA-4 blockade in melanoma. *N. Engl. J. Med.* **371**, 2189–2199 (2014).
- Van Allen, E. M. et al. Genomic correlates of response to CTLA-4 blockade in metastatic melanoma. *Science* **350**, 207–211 (2015).
- Cristescu, R. et al. Pan-tumor genomic biomarkers for PD-1 checkpoint blockade-based immunotherapy. *Science* **362**, eaar3593 (2018).
- Havel, J. J., Chowell, D. & Chan, T. A. The evolving landscape of biomarkers for checkpoint inhibitor immunotherapy. *Nat. Rev. Cancer* **19**, 133–150 (2019).
- Samstein, R. M. et al. Tumor mutational load predicts survival after immunotherapy across multiple cancer types. *Nat. Genet* **51**, 202–206 (2019).
- Marcus, L. et al. FDA approval summary: pembrolizumab for the treatment of tumor mutational burden-high solid tumors. *Clin. Cancer Res.* **27**, 4685–4689 (2021).
- Wang, Y. et al. FDA-approved and emerging next generation predictive biomarkers for immune checkpoint inhibitors in cancer patients. *Front. Oncol.* **11**, 683419 (2021).
- Chowell, D. et al. Patient HLA class I genotype influences cancer response to checkpoint blockade immunotherapy. *Science* **359**, 582–587 (2018).
- Alspach, E. et al. MHC-II neoantigens shape tumour immunity and response to immunotherapy. *Nature* 1–6. <https://doi.org/10.1038/s41586-019-1671-8> (2019).
- Axelrod, M. L., Cook, R. S., Johnson, D. B. & Balko, J. M. Biological consequences of MHC-II expression by tumor cells in cancer. *Clin. Cancer Res.* **25**, 2392–2402 (2019).
- Liu, D. et al. Integrative molecular and clinical modeling of clinical outcomes to PD1 blockade in patients with metastatic melanoma. *Nat. Med.* **25**, 1916–1927 (2019).
- Hugo, W. et al. Genomic and transcriptomic features of response to anti-PD-1 therapy in metastatic melanoma. *Cell* **165**, 35–44 (2016).
- Gide, T. N. et al. Distinct immune cell populations define response to anti-PD-1 monotherapy and anti-PD-1/Anti-CTLA-4 combined therapy. *Cancer Cell* **35**, 238–255.e6 (2019).
- Riaz, N. et al. Tumor and microenvironment evolution during immunotherapy with Nivolumab. *Cell* **171**, 934–949.e15 (2017).
- Gonzalez-Galarza, F. F. et al. Allele frequency net database (AFND) 2020 update: gold-standard data classification, open access genotype data and new query tools. *Nucleic Acids Res.* **48**, D783–D788 (2020).

24. Claeys, A., Merseburger, P., Staut, J., Marchal, K. & Van den Eynden, J. Benchmark of tools for in silico prediction of MHC class I and class II genotypes from NGS data. *BMC Genom.* **24**, 1–14 (2023).
25. Jurtz, V. et al. NetMHCpan-4.0: improved peptide–MHC class I interaction predictions integrating eluted ligand and peptide binding affinity data. *J. Immunol.* **199**, 3360–3368 (2017).
26. Nielsen, M. & Andreatta, M. NetMHCpan-3.0; improved prediction of binding to MHC class I molecules integrating information from multiple receptor and peptide length datasets. *Genome Med.* **8**, 33 (2016).
27. Rooney, M. S., Shukla, S. A., Wu, C. J., Getz, G. & Hacohen, N. Molecular and genetic properties of tumors associated with local immune cytolytic activity. *Cell* **160**, 48–61 (2015).
28. Goodman, A. M. et al. MHC-I genotype and tumor mutational burden predict response to immunotherapy. *Genome Med.* **12**, 45. <https://doi.org/10.1186/s13073-020-00743-4>.
29. Anagnostou, V. et al. Integrative tumor and immune cell multi-omic analyses predict response to immune checkpoint blockade in melanoma. *Cell Rep. Med.* **1**, 100139 (2020).
30. Campbell, K. M. et al. Prior anti-CTLA-4 therapy impacts molecular characteristics associated with anti-PD-1 response in advanced melanoma. *Cancer Cell* **41**, 791–806.e4 (2023).
31. Rodig, S. J. et al. MHC proteins confer differential sensitivity to CTLA-4 and PD-1 blockade in untreated metastatic melanoma. *Sci. Transl. Med.* **10**, eaar3342 (2018).
32. Gocher, A. M., Workman, C. J. & Vignali, D. A. A. Interferon- γ : teammate or opponent in the tumour microenvironment? *Nat. Rev. Immunol.* **22**, 158–172 (2021).
33. Claeys, A. & Van den Eynden, J. CCGlab/mhc_immunotherapy. <https://doi.org/10.5281/zenodo.12517305> (2024).

Acknowledgements

The results shown are largely based on dbGaP data with accession phs000452.v3.p1. The original work was supported by the National Human Genome Research Institute (NHGRI) Large Scale Sequencing Program, Grant U54 HG003067 to the Broad Institute. This work was supported by the Ghent University Special Research Fund Starting Grant (J.V.d.E., BOF.STG.2019.0073.01, <https://www.ugent.be/en/research/funding/bof>) and Kom op tegen Kanker (Stand up to Cancer), the Flemish cancer society (AC; STI.VLK.2022.0013.01). The funders had no role in study design, data collection and analysis, decision to publish, or preparation of the manuscript.

Author contributions

J.V.d.E. conceptualized the study. A.C. and J.V.d.E. acquired the data and performed the analyses. J.V.d.E. wrote the manuscript. All authors read, revised and approved the manuscript.

Competing interests

The authors declare no competing interests.

Additional information

Supplementary information The online version contains supplementary material available at <https://doi.org/10.1038/s43856-024-00612-w>.

Correspondence and requests for materials should be addressed to Jimmy Van den Eynden.

Peer review information *Communications Medicine* thanks the anonymous reviewers for their contribution to the peer review of this work. Peer reviewer reports are available.

Reprints and permissions information is available at <http://www.nature.com/reprints>

Publisher's note Springer Nature remains neutral with regard to jurisdictional claims in published maps and institutional affiliations.

Open Access This article is licensed under a Creative Commons Attribution-NonCommercial-NoDerivatives 4.0 International License, which permits any non-commercial use, sharing, distribution and reproduction in any medium or format, as long as you give appropriate credit to the original author(s) and the source, provide a link to the Creative Commons licence, and indicate if you modified the licensed material. You do not have permission under this licence to share adapted material derived from this article or parts of it. The images or other third party material in this article are included in the article's Creative Commons licence, unless indicated otherwise in a credit line to the material. If material is not included in the article's Creative Commons licence and your intended use is not permitted by statutory regulation or exceeds the permitted use, you will need to obtain permission directly from the copyright holder. To view a copy of this licence, visit <http://creativecommons.org/licenses/by-nc-nd/4.0/>.

© The Author(s) 2024